Mansoura Journal of Chemistry Vol. 35 (2), December, 2008.

THE EFFECT OF METAL LOADING ON THE STRUCTURE AND ACTIVITY OF HYDROTREATING CATALYST

M. G. Abd El-Wahed [a], F. Y. A. El Kady [b], S.A. Shaban [b] and A. M. Osama [b, *]

[a]Department of Chemistry, Faculty of Science, Zagazig University, Zagazig, Egypt.

[b]Catalysis Department, Refining Division, Egyptian Petroleum Research Institute, Nasr City, Cairo 11727, Egypt.

(Received: 12 / 10 / 2008)

ABSTRACT

Incipient wetness impregnation technique has been used to determine the molybdenum oxide content that would cover the entire surface of the γ-alumina support with a single monolayer. For this purpose, a series of unpromoted molybdenum containing catalyst supported on γ-alumina with different MoO_3 loading, ranging from 0 to 36 wt% was prepared.

XRD, IR spectroscopy, nitrogen adsorption-desorption isotherms and cyclohexene dehydrogenation were used to assess the structural properties and catalytic activities of the prepared catalysts. The dispersion capacity of MoO_3 on the surface of γ-alumina can be measured also by XRD quantitative phase analysis and specific surface area. The results indicate that the dispersion capacity of molybdenum on γ-alumina is about 4.95 Mo atom/nm^2.

Keywords: Infrared spectroscopy (IR); Surface properties; X-ray diffraction; monolayers.

1-INTRODUCTION

Recently the stringent environmental regulations established high quality transportation fuel specification to reduce automobile emissions and to minimize the environmental pollution. The sulphur content in diesel has been implemented to be lowered to or less than 50 ppm since 2005. To meet this assignment, more attention is being made for product

upgrading via deep or ultra deep hydrodesulphurization (HDS) of diesel **[Kallinikos et al., (2008) and Duan et al., (2007)].**

Conventional hydrotreating catalysts are based on Mo or W supported on alumina and they are frequently promoted with Co or Ni **[Linares et al., (2008)].**The influence of the metal loading i.e., Mo (W) and Co (Ni), on the structure and activity of hydrotreating catalyst has been the subject of numerous studies **[De Beer et al., (1976); Okamoto et al., (1980); Chung & Massoth (1980); Wang & Hall (1982); Li & Hercules (1984); Arnoldy et al., (1985); Gosselink et al., (1987); Van Veen et al., (1992); Shimada et al., (1993) and Topsøe et al., (1996)].** Although from a commercial point of view the highest activity/selectivity on a catalyst volume basis is the most important criterion, also the metal utilization plays a decisive role. Obviously, one goal is the formation of the maximum possible amount of Co-Mo-S type phases without wasting metals in less active or inactive bulk structures.

For molybdena/ alumina catalysts, loading of molybdenum lower than that corresponding to monolayer, was found to be more difficult to sulfide than in high loading catalysts, as revealed by chemical analyses **[De Beer et al., (1976)]**, XPS **[Li & Hercules (1984) and Okamoto et al., (1980)]**, EXAFS **[Shimada et al., (1993)]**, and TPS studies **[Arnoldy et al., (1985)]**. This is due to the interaction of molybdenum with the alumina basic hydroxyl groups in the oxidic precursor. After sulfidation, MoS_2 species remain bonded to the alumina surface via a few oxygen bonds (Mo-O-Al linkages), decreasing the HDS activity **[Topsøe et al., (1996)]**.

Well dispersed octahedral cobalt on γ-alumina and/or molybdenum phase surface, which is easily reduced and/or sulfided, participates in the formation of HDS active sites **[Papadopoulou et al., (2004); Van Veen et al., (1992); Arnoldy et al., (1985); Wivel et al., (1984) and Topsøe & Topsøe (1982)].** At the Mo loading lower than that corresponding to monolayer, the capacity of the support for the dispersion of Mo species is not fully utilized and the uncovered alumina surface will interact with Co^{+2} ions forming $CoAl_2O_4$ (inactive phase). While, the formation of monolayer over the support surface gives no opportunity for Co^{+2} ions to find uncovered γ-alumina to form $CoAl_2O_4$and hence maximum activity is obtained.

Above the monolayer, separate MoO_3 entities are formed, resulting in bulk-like MoS_2 phases upon sulfidation **[Van Veen et al., (1992) and Gosselink et al., (1987)]**. The consequence is that the

edge/basal plane ratio of the MoS_2 phase is decreased resulting in a lower activity and less edge sites available to accommodate the promoter ions. Thus, the optimum molybdenum loading for HDS is at or near the monolayer loading.

The aim of this paper is to determine the molybdenum oxide content that would cover the entire surface of the γ-alumina support with a single monolayer **(monolayer loading)**. For this purpose, a series of unpromoted molybdenum containing catalyst supported on γ-alumina with different MoO_3 loadings was prepared by the incipient wetness impregnation technique using ammonium heptamolybdate (AHM) as a precursor salt of molybdenum oxide. The structural prosperities of the catalyst were assessed by XRD, IR spectroscopy and N_2 adsorption-desorption isotherm. The catalytic activity of the prepared catalysts was determined through cyclohexene dehydrogenation reaction.

2. EXPERIMENTAL

2.1. Support / Catalyst Preparation

2.1.1. Support Preparation

The γ-Al_2O_3 support was prepared by calcinating boehmite in air at 550°C for 5 h. The Brunauer–Emmett–Teller (BET) surface area of the γ-Al_2O_3 was 162.88 m^2/g. The support was activated at 550°C for 2 h before being used in the catalyst preparation to eliminate adsorbed organic impurities.

2.1.2. Catalyst Preparation

Catalyst samples were prepared by impregnation of the □-Al_2O_3 supports with aqueous solutions of ammonium heptamolybdate through incipient-wetness impregnation method. After impregnation; the moist paste was preliminary dried in an oven at 120°C over night and then calcined in a muffle furnace at 450°C for 4 h.

Molybdenum supported catalysts were denoted by x MoAl where x is the loading corresponding to MoO_3 .i.e., 4 MoAl refers to a sample of MoO_3 supported on γ-Al_2O_3 having 4 % of the active element as MoO_3. The nominal molybdenum oxide loadings were varied in the range of 4-36 wt%.

2.2. Catalyst Characterization

2.2.1. Chemical Analysis

Atomic absorption spectroscopy (AAS) was carried out in a spectrometer using C_2H_2–NO_2 flame (3000°C) for checking the real Mo content of the catalysts. For complete dissolution the samples were digested by acid treatment with H_2SO_4 and HF at 200°C and 15–20 kg/cm^2 for 20 min, on a CEM-Mars 5 microwave oven.

2.2.2. X-ray diffraction (XRD)

X-ray powder diffraction patterns (XRD) were performed at room temperature on a Philips model pw 1050 diffractometer using a Ni filtered Cu Kα (wavelength λ= 1.540 Å) radiation source operating at a capacity of 30 kV and a current of 40 mA and a scanning range 2θ of 18–80° at a rate of 8° min^{-1}. The XRD phases present in the samples were identified with the help of the Joint Committee of Powder Diffraction Standards **(JCPDS)** powder data files.

2.2.3. Textural Analysis

The textural parameters including surface area and pore structure of the different samples were studied by isothermal adsorption of nitrogen at 77 K using Quantachrome Nova 3200 S automates gas sorption apparatus. Prior to any adsorption measurement the sample was degassed at 350°C for 3 h under a reduced pressure of 10^{-5} Torr. The specific surface areas (S_{BET}, m^2/g) of the samples were calculated according to the standard Brunauer, Emmett and Teller (BET) procedure using nitrogen adsorption data collected in the relative equilibrium pressure interval of 0.05 < P/Po < 0.35, where linear relationship was maintained. The monolayer capacity was determined and S_{BET} was calculated adopting 0.162 nm^2 as the cross-sectional area of the adsorbed nitrogen molecule. The total pore volume (V_p, ml/g) was estimated from the maximum mount of nitrogen adsorbed at STP, from the desorption branch of the isotherm at the relative pressure close to unity assuming complete pore saturation and are expressed in ml g^{-1}. The average pore diameters (d_p, nm) of all the catalysts were calculated following a simple relation between the BET surface area and the total pore volume assuming an open-ended cylindrical pore model without pore networks:

$$d_p = \frac{4 \times pore\ volume\ \left(ml\,g^{-1}\right) \times 1000}{Surface\ area\ \left(m^2 g^{-1}\right)}$$

The t-plot method was used for analyzing microporosity in the catalyst.

2.2.4. Infrared Spectroscopy

To obtain detailed information about the molecular structure of the supported catalysts, the IR transmission spectroscopic investigation was carried out at room temperature on Mattson 8100.spectrometer using KBr disc method. IR data were collected by averaging 32 scans with a spectral resolution of 4 cm^{-1} over the wave number range of 400-1200 cm^{-1}.

2.3. Catalyst Activity Assessment

The dehydrogenation reaction of cyclohexene was used to assess the catalytic activity of the various solid catalyst samples. The reaction was carried out in microcatalytic pulse reactor made up of stainless steal (25 cm long and 8 mm i.d.) placed in an electrically heated oven, operating at atmospheric pressure **(Figure 1)**. About 0.29 g of catalyst sample mixed with 0.1 g of inert glass particles of the same particle size as that of the catalyst was placed at the center of the microcatalytic reactor and kept in position by a thin layer of quartz wool on both sides. Prior to catalytic activity test, the catalyst samples were activated "in situ" by heating at 400°C for 2 h in a flow of nitrogen of 50 ml/min. The catalytic measurements were performed by injecting a constant dose of 1 µl cyclohexene using a micro-syringe into the micro-reactor bed. To ensure the sample pulsed to gasify quickly and completely, the temperature at sampling inlet was controlled at 250°C. Ultrapure nitrogen gas, deoxygenated and dried by molecular sieves, was employed as a carrier in the reactions under study, at a flow rate of 50 ml/min. The dehydrogenation activities of molybdena supported catalysts were estimated by varying the temperature from 200 to 400°C, with 50°C decrements starting from 400°C downwards. The reactor temperature was regulated by means of a variable transformer and monitored by chromel – alumel thermocouple while the flow of the carrier gas was controlled by mass flow meter.

Analyses:

Product analysis was performed on-line with a Perkin Elmer Sigma 3 M gas chromatograph, with flame ionization detector (FID) and equipped with a column made of a stainless steel cylinder of 3 mm inside diameter and 4 m long and packed with h 5 wt% Bentone-34 and 5 wt%

di- isodecyl - phthalate on chemsorb 35-80 mesh. The chromatographic column temperature was adjusted and controlled at 70°C. Products were identified by comparison with authentic samples.

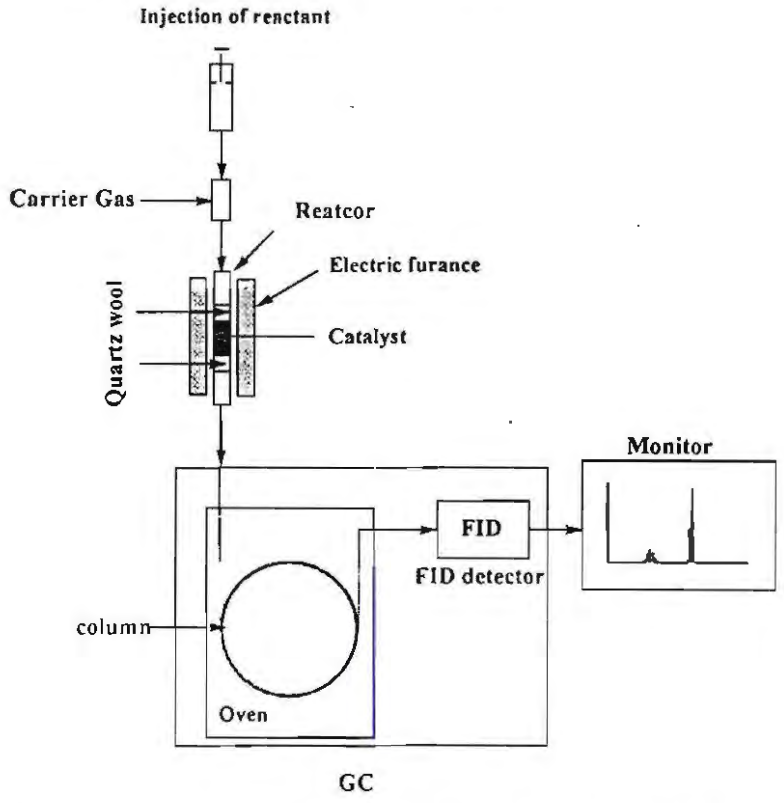

Fig. (1): Schematic diagram of the microcatalytic pulse reactor.
GC, gas chromatograph; *FID*, flame ionization detector

3. RESULTS AND DISCUSSION

3.1. Chemical Analysis

Chemical analysis results **Table 1** show that the actual chemical compositions (Mo loading) of the prepared x-Mo/γ-Al_2O_3 catalysts are close to the expected nominal ones.

The Molybdenum surface densities are expressed as the number of Mo atoms per square nanometer (Mo atoms/nm^2) **[Chen et al., (2000)]**. They are calculated using the following equation and are listed in **Table 1**.

Table (1): Chemical composition of the Mo/Al_2O_3 series with various MoO_3 loadings.

Solid Catalyst	Mo Loading (wt. %)		Mo Surface Density (Mo/nm^2)
	Nominal	Actual (AAS* Analysis)	
γ-Al_2O_3	0	0	0
4 MoAl	4	3.8	1.06
8 MoAl	8	7.9	2.26
12 MoAl	12	11.7	3.58
16 MoAl	16	15.8	4.95
20 MoAl	20	19.8	7.15
24 MoAl	24	23.7	9.65
28 MoAl	28	27.9	12.48
32 MoAl	32	31.8	15.74
36 MoAl	36	35.8	18.81

* **AAS:** atomic absorption spectroscopy.

$$Mo\ surface density = \frac{MoO_3\ percentage \times Avogadreos\ number\left(6.02\times10^{23}\right)}{surface area\left(m^2\ g^{-1}\right)\times Molecular weight of\ MoO_3\left(144\ g\ mol^{-1}\right)\times10^{18}}$$

Where: 10^{18} is a conversion factor

3.2. X-ray diffraction analysis

The X-ray powder diffraction analysis was undertaken to determine the composition and crystallinity of Mo species in $MoO_3/\ \gamma$-Al_2O_3. Powder X-ray diffractograms of the alumina-supported molybdenum oxide catalysts are presented in **Figure 2**. Inspection of **Figure 2** reveals that all samples exhibited broad peaks corresponding to microcrystalline γ-Al_2O_3 support **(JCPDS file no. 10-425)**. No diffraction lines corresponding to molybdenum containing compounds were detected in samples with MoO_3 loading up to 4.95 Mo atom/ nm^2 (16 wt% MoO_3), indicating that molybdenum species were either highly dispersed or present as MoO_3 crystallites having sizes less than 4 nm, which is beyond the detection capacity of XRD. To the contrary, higher

MoO_3 loadings led to the appearance of diffraction lines at 2θ of 27.3, 25.7, and 23.3 attributed to the (021), (040) and (110) phases of the orthorhombic MoO_3 phase (**JCPDS file no. 35-609**). The intensity of these lines increases with the molybdena loadings.

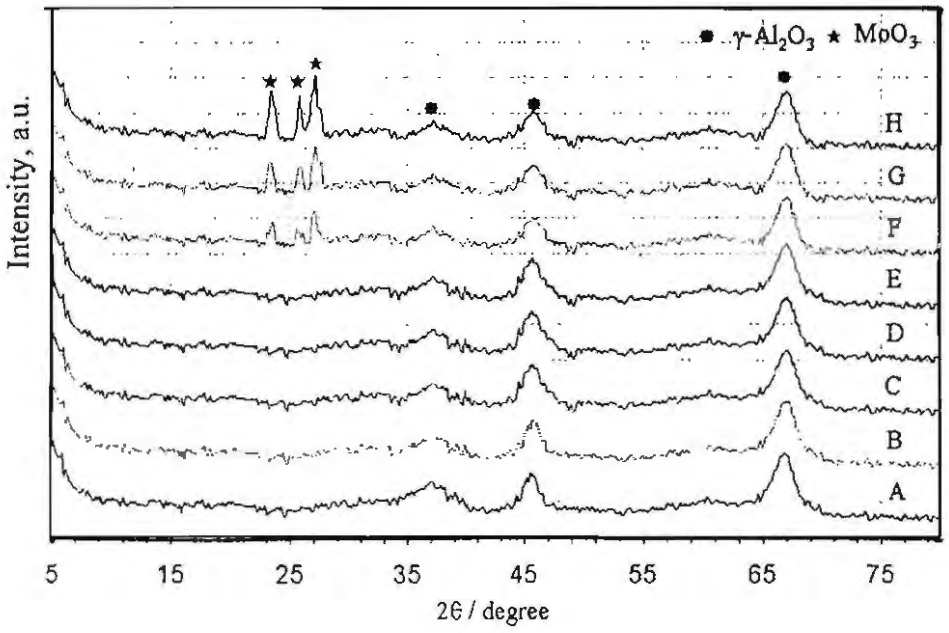

Fig. (2): X-ray diffraction patterns of MoO_3/γ-Al_2O_3 catalysts with different molybdenum surface density.
A: γ-alumina, **B**: 4 MoAl, **C**: 8 MoAl, **D**: 12 MoAl, **E**: 16 MoAl, **F**: 20 MoAl, **G**: 24 MoAl, **H**: 28 MoAl.

The dispersion capacity of MoO_3 on the surface of γ-Al_2O_3 could be measured by XRD quantitative phase analysis. XRD quantitative analysis was carried out by plotting the area ratio of crystalline MoO_3 peak at 27.3° and support peak at 67° (I_{MoO3}/I_{Al2O3}) as a function of MoO_3 surface density. The resultant straight line gives an intercept with the horizontal axis corresponding to the dispersion capacity of MoO_3 on the surface of γ-Al_2O_3 **[Wang et al., (1999); Xie & Tang (1990) and Liu et al., (1982)]**. The result indicates that the dispersion capacity of molybdena on γ-Al_2O_3 is about 4.95 Mo atom/nm^2 as shown in **Figure 3**. This result agrees with previous results where the Mo surface density corresponding to monolayer on γ-Al_2O_3 support has been reported to be

~5 Mo atom/nm^2 [**Tsilomelekis et al., (2007); Christodoulakis et al., (2006) and Xie et al., (2000)**]. The calculated theoretical monolayer coverage based on the effective ionic diameter of MoO_6 octahedral is 4.9 Mo/nm^2 [**Edwards et al., (1990)**], while molybdena monolayers of tetrahedral and octahedral coordination for loadings of up to 7 Mo/nm^2 have also been reported [**Matsuoka et al., (1990)**].

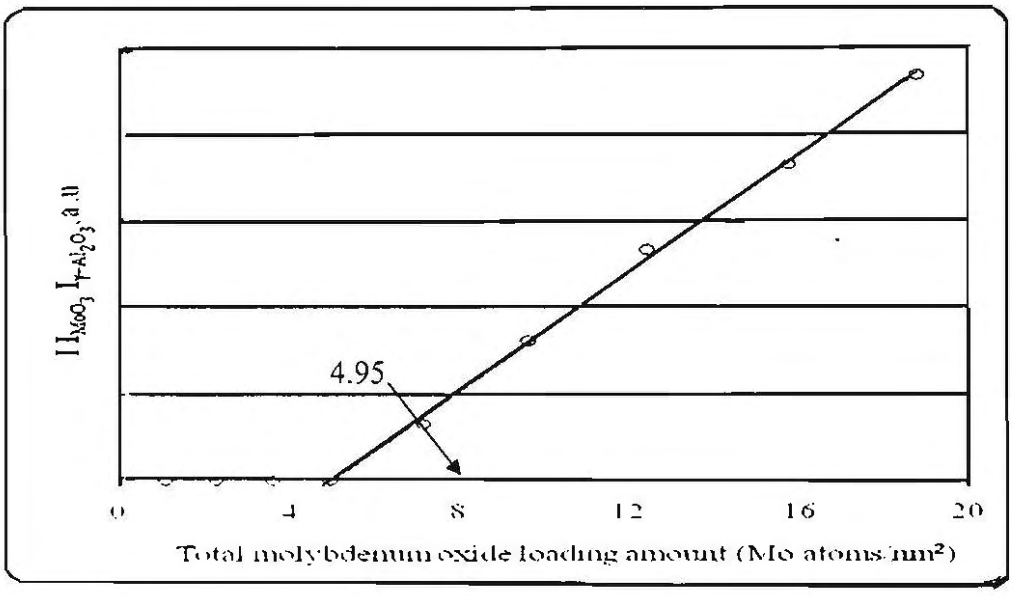

Fig.(3): Determination of dispersion capacities of MoO_3 on γ-Al_2O_3 through quantitative XRD.

3.3. IR analysis

The IR spectra of molybdenum oxide supported on alumina catalysts were carried out using KBr pellets. The final spectra were taken after 32 scans with 4 cm^{-1} resolution. The spectrograms as a function of Mo-loadings are shown in **Figure 4**. In IR spectra, 800–1200 cm^{-1} region is interesting as in this region characteristic bands due molybdenum species can be detected. Inspection of **Figure 4** reveals that:

- For 4 Mo/γ-Al_2O_3 sample, the band at 914 cm^{-1} characterizes the stretching mode of Mo=O bond in surface-bound Mo species. These species may be either isolated tetrahedral or octahedral polymolybdate species. The absence of a band due to bridged Mo–O–Mo bonds in the lower wave number region indicates that

these species are isolated tetrahedral species **[Imamura et al., (1998); Mortimer et al., (1993) and Giordano et al., (1975)].**

- For catalyst samples 8 Mo/γ-Al_2O_3, 12 Mo/γ-Al_2O_3 and 16 Mo/γ-Al_2O_3, the band due to Mo=O stretching becomes at 950 cm^{-1}. The appearance of a new band at 650 cm^{-1} which ascribes to the characteristic bridged Mo–O–Mo bonds indicates the formation of octahedral polymolybdate species in addition to the isolated tetrahedral species **[Mortimer et al., (1993)]**. The increase in the intensity of this band with MoO_3 loading inidicates the growth of the ploymolybdate species.
- At higher loadings, the bands due to microcrystallites MoO_3 appears at 600, 830 and 880 cm^{-1} **[Imamura et al., (1998)]**. The intensity of these bands increases with increasing molybdenum loading. These results are in line with XRD analysis, which indicates the formation of microcrystallites MoO_3 at Mo loadings exceeding monolayer content.

Based on IR results, upon increasing the MoO_3 loading, three types of species are identified, i.e.:

- At low molybdena loading, isolated tetrahedral molybdenum species exist.
- At higher molybdena loading, but still lower than that corresponding to monolayer coverage, octahedral polymolybdate species characterized by bands at 950 and 650 c^{m-1} exist in addition to isolated tetrahedral molybdenum species.
- At molybdenum loadings exceeding monolayer, microcrystallites MoO_3, characterized by bands at 600, 830 and 880 cm^{-1}, begins to be formed and its amount increases with further increase in Mo loading.

A scheme of the formation of this species can be ascribed as following:

Mo is present in the forms of heptamolybdate $(Mo_7O_{24})^{-6}$ and monomeric MoO_4^{2-} at an equilibrium in an aqueous phase solution **[Imamura et al., (1998) and Vit & Zdrazil (1997)]:**

$$Mo_7O_{24}^{-6} + 4\,H_2O \longrightarrow MoO_4^{-2} + 8\,H^+$$

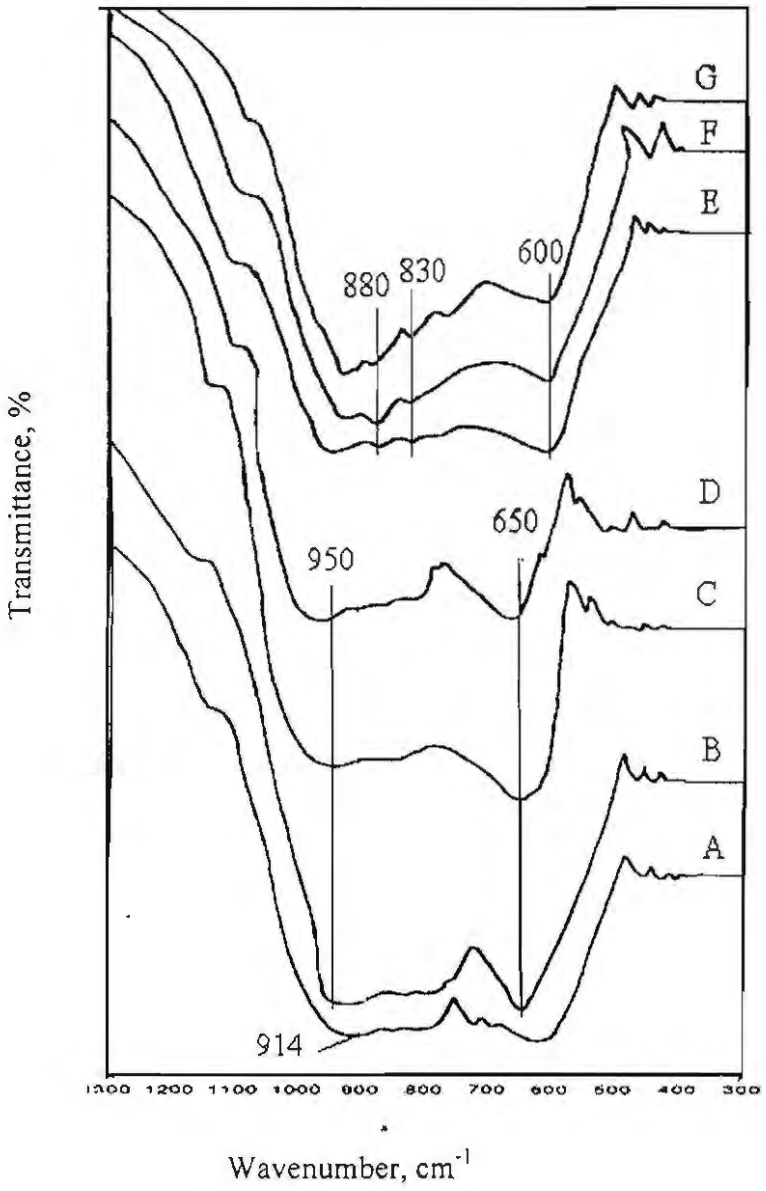

Fig. (4): IR spectrograms as a function of Mo-loadings.
A: 4 MoAl, **B:** 8 MoAl, **C:** 12 MoAl, **D:** 16 MoAl, **E:** 20 MoAl, **F:** 24 MoAl, **G:** 28 MoAl.

At low molybdenum loading, monomeric MoO_4^{2-} is preferentially adsorbed (exchanged) on the basic hydroxyl groups present on alumina and, thus, isolated tetrahedral species are formed **[Vit (1999) and Diaz & Bussell (1993)]**.

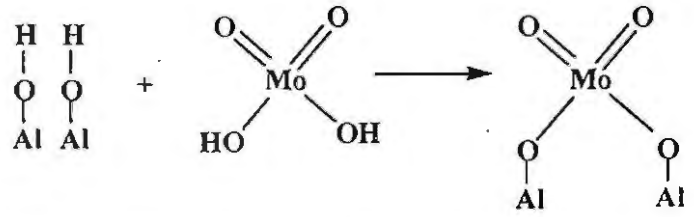

At higher Mo loading, the consumption of the OH in the support continuously diminished and the OH/ Mo stoichiometry was smaller due to overwhelming formation of polymolybdate species **[Vit (1999) and Vit & Zdrazil (1997)]**.

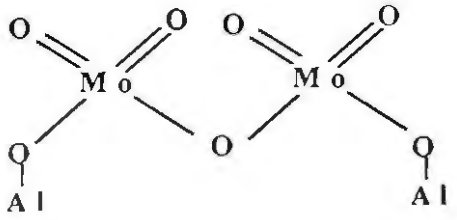

OH/Mo = 1

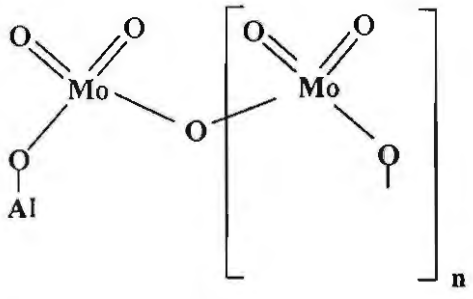

OH/Mo < 1

A further increase of the molybdenum loading (> monolayer) resulting in decrease in the interaction between the molybdenum species and the alumina support leads to the formation of three-dimensional aggregates of MoO_3 **[Barath et al., (1999)]**.

3.4. Textural Properties

The nitrogen adsorption-desorption isotherms of γ-Al_2O_3 and x Mo/γ-Al_2O_3 catalysts are shown in **Figure 5**. All the isotherms are of type IV of the IUPAC classification and showed a characteristic hysteresis loops indicating capillary condensation in mesopores **Figure 5**. A progressive decrease in the amount of the adsorbed N_2 is observed with an increase in MoO_3 loading.

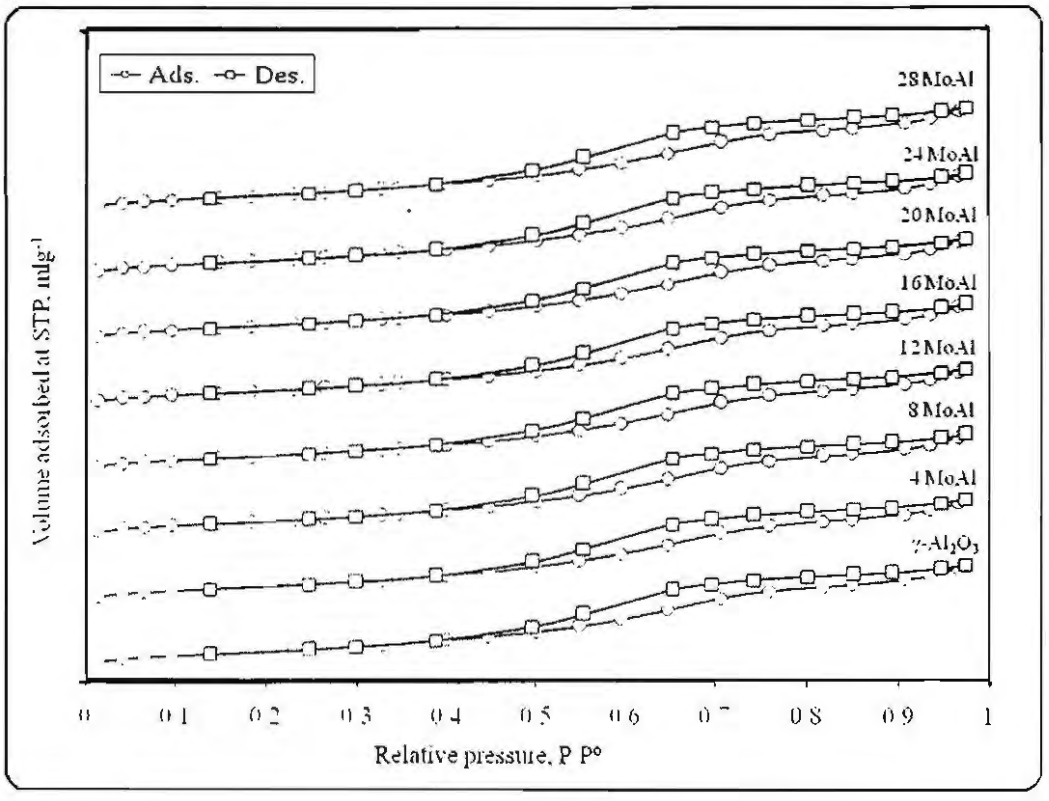

Fig.(5): Nitrogen adsorption-desorption isotherms of MoO_3/γ-Al_2O_3 catalysts with different molybdenum surface density.

The specific surface areas listed in **Table 3** were determined by the application of the Brunauer–Emmett–Teller (BET) method. The BET plots (not illustrated) show excellent linearity, with a correlation factor of 0.9999. Specific surface area is not only useful to know the extent of surface available for the dispersion of the active component but also to assess if the active component is dispersed as a monolayer or not

[Murali Dhar et al., (2005)]. Normally, when monolayer formation is taking place the surface area per gram of catalyst decreases, whereas surface area per gram of support remains constant as a function of Mo content and as soon as the monolayer is completed the surface area decreases with a further increase of molybdenum loading **[Murali Dhar et al., (2005); Chiranjeevi et al., (2002) and Maity et al., (2001)]**. Figure 6 depicts the variation of the surface area per gram of support and per gram of catalyst as a function of molybdenum loading. Figure 6 depicts that surface area per gram of support remains constant up to 4.95 Mo atom per nm^2 (16 wt% MoO_3) and then it decreases. The variation of pore volume as a function of Mo loading is also presented in **Figure 6**. It is noted that pore volume decreases with molybdenum loading but the decrease is not significant up to 16 wt.% whereas, sharp decrease is exihibited at higher loadings. Therefore, it appears form surface area and pore volume results that molybdenum is well dispersed as a monolayer up to 16 wt%.

It is evident that the XRD results are in good agreement with the surface area results. Thus, the absence of crystalline Mo species up to 4.95 atom/nm^2 may be related to the approximately constant surface area. Beyond this value, crystallization seems to be associated with a pronounced decrease of the surface area.

Table (2): XRD phases of MoO_3 / γ-Al_2O_3 catalysts with different MoO_3 loadings.

Solid Catalysts	XRD crystalline phases (*)
4 MoAl	γ-Al_2O_3 **(10-425)**
8 MoAl	γ-Al_2O_3 **(10-425)**
12 MoAl	γ-Al_2O_3 **(10-425)**
16 MoAl	γ-Al_2O_3 **(10-425)**
20 MoAl	γ-Al_2O_3 **(10-425)** + MoO_3 **(35-609)**
24 MoAl	γ-Al_2O_3 **(10-425)** + MoO_3 **(35-609)**
28 MoAl	γ-Al_2O_3 **(10-425)** + MoO_3 **(35-609)**
32 MoAl	γ-Al_2O_3 **(10-425)** + MoO_3 **(35-609)**
36 MoAl	γ-Al_2O_3 **(10-425)** + MoO_3 **(35-609)**

* XRD phases present in the samples were identified with the help of JCPDS Powder Data Files.

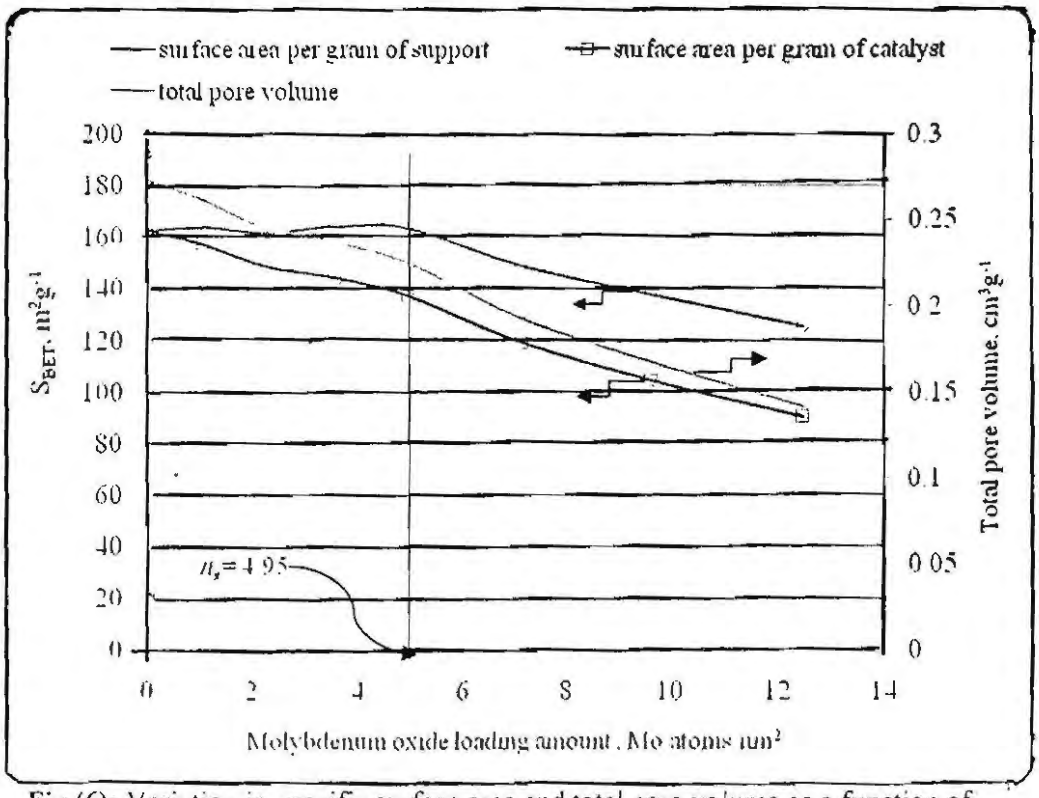

Fig.(6): Variation in specific surface area and total pore volume as a function of Mo surface density (Mo atom/nm^2).

The *V–t* plots **Figure 7** show two steps, the highest (an upward deviation from the linear branch of the t plot with ascending t values) corresponding to capillary condensation (which starts at relative pressures similar to those of the corresponding hysteresis loops) and the lowest (linear t plot passing through the origin) corresponding to a mono-multi- layer adsorption mechanism on pores in which the adsorption - desorption was reversible, thus confirming the mesoporous texture of the solids and the absence of microporosity. The specific surface areas calculated from *V–t* plot from the slopes of the straight lines (**Table 3**) were found to be in a good agreement with those evaluated by the *BET* method.

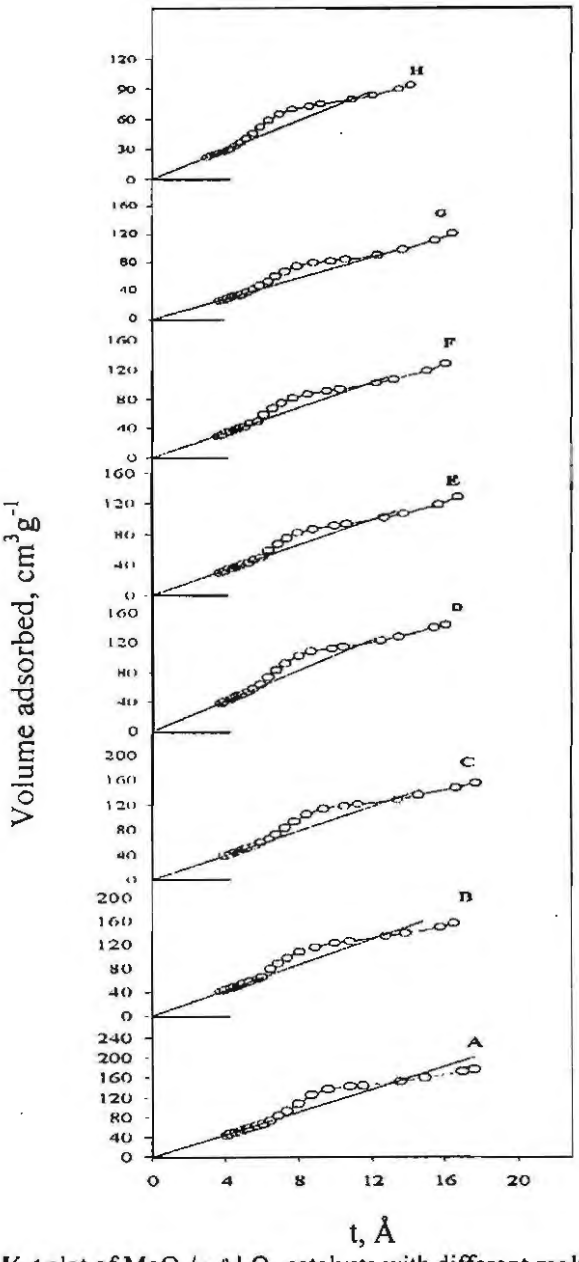

Fig.(7): *V–t* plot of MoO_3/γ-Al_2O_3 catalysts with different molybdenum surface density
A: γ-alumina, **B**: 4 MoAl, **C**: 8 MoAl, **D**: 12 MoAl, **E**: 16 MoAl,
F: 20 MoAl, **G**: 24 MoAl, **H**: 28 MoAl.

Table (3): Textural properties of the γ-Al_2O_3 support and of MoO_3 / γ-Al_2O_3 catalysts with different MoO_3 loadings as determined from nitrogen adsorption-desorption isotherms.

Solid Catalyst	S_{BET}		V_p (mlg^{-1})	d_p (nm)	S_t (m^2 g^{-1})
	(m^2 g^{-1} $_{cat.}$)	(m^2 g^{-1} $_{supp.}$)			
γ-Al_2O_3	162.88	162.88	0.2732	6.709	162.88
4 MoAl	157.29	163.84	0.261652	6.654	157.29
8 MoAl	148.81	161.75	0.245388	6.596	148.81
12 MoAl	144.52	164.22	0.237085	6.562	144.52
16 MoAl	137.45	163.63	0.225212	6.554	137.45
20 MoAl	119.14	148.92	0.19259	6.466	119.14
24 MoAl	104.6	137.63	0.167569	6.408	104.6
28 MoAl	90.21	125.29	0.141255	6.278	90.21

V_p: total pore volume; d_p: average pore diameter, and S_t: surface area derived from *V-t* plot.

3.5. Catalytic Activity

Figure 8 depicts the behavior of the current catalysts towards cyclohexene dehydrogenation to benzene as a function of reaction temperature. Cyclohexene dehydrogenation is an endothermic reaction, thus requiring high temperatures. Evidently, benzene production continually increases as a function of reaction temperature using all current catalysts.

Figure 9 represents the yield of benzene at constant reaction temperature as a function of molybdenum loading. It can be seen that, dehydrogenation activity for xMoAL catalysts with different MoO_3 loadings increases up to 4.95 Mo atom/ nm^2 (corresponding to 16 wt% MoO_3) and then decreases with further increase of Mo loading. This shows that monolayer loading [4.95 Mo atom/nm^2 (16 wt %)] is the optimum loading to obtain maximum activity for dehydrogenation reaction. Theses results are in agreement with previous studies concerning the effect of the molybdenum content on the catalytic activity of molybdena supported catalysts in a vast number of catalytic reactions **[Wang et al., 1999].**

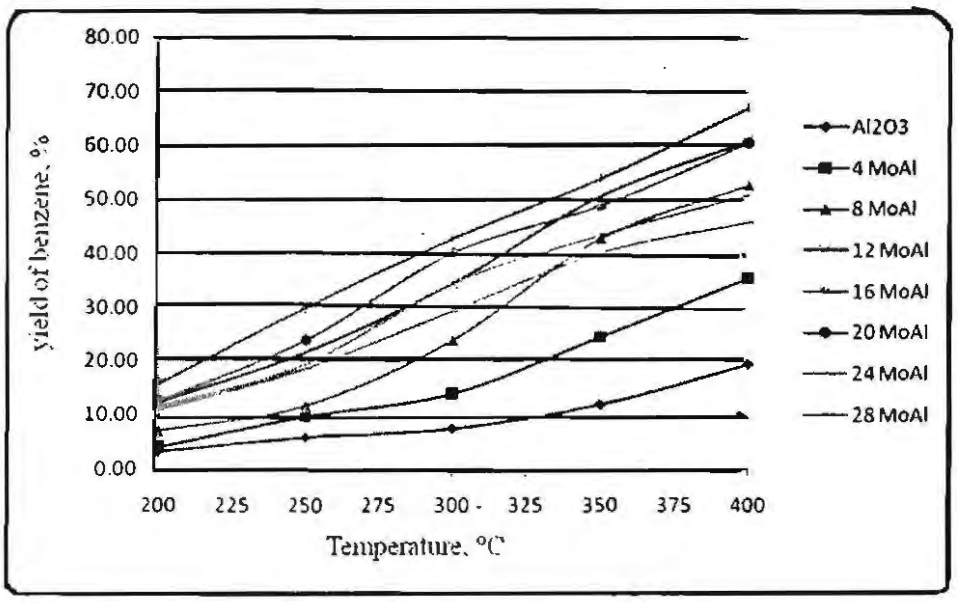

Fig.(8): Effect of temperature on the yield of benzene using MoO_3/γ-Al_2O_3 catalysts with different molybdenum surface density.

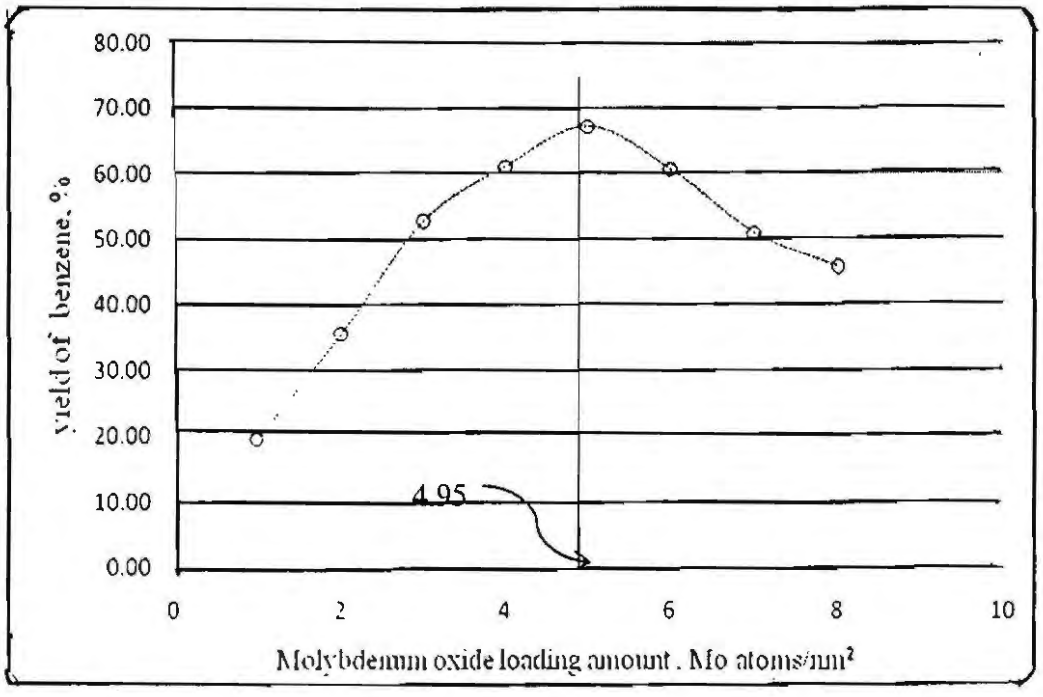

Fig.(9): Variation of the benzene yield as a function of molybdenum surface density at 400°C.

4. CONCLUSIONS

The following are the main conclusions that may be drawn from the obtained results:

1. XRD results indicate that molybdenum oxide species are dispersed as a monolayer on the support up to 16 wt.% Mo and the formation of crystalline MoO_3 is observed above this loading.
2. IR results showed that molybdenum oxide species were present predominantly in tetrahedral form at lower loading and polymeric octahedral forms dominate, at higher loading. At molybdenum loadings higher than monolayer loadings MoO_3 microcrystallites are detected.
3. Cyclohexene dehydrogenation to benzene was found to increase with increasing Mo loading up to 16 wt. % (monolayer loading) and then decreased with further increase in loading.

REFERENCES

Arnoldy, P. Van den Heijkant, J.A.M. De Book, G.D. Moulijn, J.A. J. Catal. 35 (1985) 92.

Barath, F. Turki, M. Keller1, V. Maire, G. J. Catal. 185 (1999) 1.

Chen, K. Xie, S. Iglesia, E. Bell, A.T. J. Catal. 189 (2000) 421.

Chiranjeevi, T. Kumar, P. Rana, M.S. Murali Dhar, G. Prasada Rao, T.S.R. J. Mol. Catal. A: Chem. 181 (2002) 109.

Christodoulakis, A. Heracleous, E. Lemonidou, A.A. Boghosian, S. J. Catal. 242 (2006) 16.

Chung, K.S. and Massoth, F.E. J. Catal. 64 (1980) 320.

De Beer, V.H.J. Van der Aalst, M.J.M. Machiels, C.J. Schuit, G.C.A. J. Catal. 43 (1976) 78.

Diaz, A. L. and Bussell, E. J. Phys. Chem. 97 (1993) 470.

Duan, A. Wan, G. Zhao, Z. Xu, C. Zheng, Y. Zhang, Y. Dou, T. Bao, X. Chung, K. Catal. Today, 119 (2007) 13.

Edwards, J.C. and Adams, R.D. Ellis, P.D. J. Am. Chem. Soc. 112 (1990) 8.

Giordano, N. Bart, J. C. J. Vaghi, A. Castellan, A. Martinotti, G. J. Catal. 36 (1975) 81.

Gosselink, J.W. Schape, H. De Jong, J.P. Stor, W.H.J. Appl. Catal. 32, (1987) 337.

Imamura, S. Sasaki, H. Shono, M. Kanaiy, H. J. Catal. 177 (1998) 72.

Kallinikos, L.E. Bellos, G.D. Papayannakos, N.G. fuel 87 (2008) 2444.

Li, C.P. Hercules, and D.M. J. Phys. Chem. 88 (1984) 456.

Linares, C. F. Amézqueta, P. Scott, C. fuel 87 (2008) 2817.

Liu, Y.J. Xie, Y.C. Ming, J. Liu, J. Tang, Y.Q. J. Catal.(China) 3 (1982) 262.

Maity, S.K. Rana, M.S. Bej, S.K. Ancheyta-Juárez, J. Murali Dhar, G. Prasada Rao, T.S.R. Appl. Catal. A: General 205 (2001) 215.

Matsuoka, Y. Niwa, M. Murakami, Y. J. Phys. Chem. 94 (1990) 1477349.

Mortimer, R. Powell, J. G. Greenblatt, M. McCarroll, W. H. Ramanujachary, K.V. J.Chem. Soc., Faraday Trans. 89, (1993) 3603.

Murali Dhar, G. Muthu Kumarana, G. Kumara, M. Rawata, K.S. Sharmaa, L.D. David Rajub, B. Rama Rao, K.S. Catal. Today 99 (2005) 309.

Okamoto, Y. Tomioka, H. Imanaka, T. Teranishi, S. in: Seiyma, T. Tanabe, K. (Eds) Proc. 7th Int. Congr.Catal.. Elsevier, Amsterdam, 1980, p. 616.

Papadopoulou, Ch. Vakros, J. Matralis, H. K. Voyiatzis, G. A. Kordulis, Ch. J. of Colloid. Interf. Sci. 274 (2004) 159.

Shimada, H. Matsubayahi, N. Sato, T. Yoshimura, Y. Imamura, M. Kameoka, T. and Nishijima, A. Catal. Lett. 81 (1993) 20.

Topsøe, H. Clausen, B.S. Massoth, F.E. Hydrotreating catalysis Springer, Berlin, 1996.

Topsøe, N.Y. and Topsøe, H. J. Catal. 77 (1982) 293.

Tsilomelekis, G. Christodoulakis, A. Boghosian, S. Catal. Today 127 (2007) 139.

Van Veen, J.A.R. Gerkema, E. Van der Kraan, A.M. Hendriks, P.A.J.M. Beens, H. J. Catal. 133 (1992) 112.
Vit, Z. and Zdrazil, M. J. Catal. 171 (1997) 305.

Vit, Z. Surface and interface analysis, 24 (1999) 861.

Wang, L. Hall, W.K. J. Catal. 77 (1982) 232.

Wang, X. Zhao, B. Jiang, D. Xie, Y. Appl. Catal. A: General 188 (1999) 201.

Wivel, C. Candia, R. Clausen, B.S. Morup, S. Topsøe, H. J. Catal. 87 (1984) 497.

Xie, Y.C. and Tang, Y.Q. Adv. Catal. 37 (1990) 1.

Xie, S. Chen, K. Bell, A.T. Iglesia, E. J. Phys. Chem. B 104 (2000) 10059.

تأثير نسبة المعدن علي تركيب ونشاطية حفاز المعالجة الهيدروجينية

محمد جمال عبد الواحد، فتحي يوسف القاضي، سهام علي شعبان واحمد محمد أسامة

تم استخدام طريقة التشرب (incipient wetness impregnation) لتحديد نسبة اوكسيد المولبدنم (MoO_3) اللازمة لتغطية سطح الالومينا بطبقة أحادية (Single monolayer). ولهذا الغرض تم تحضير سلسلة من حفاز اوكسيد المولبدنم المحمل علي الالومينا بنسب مختلفة من اوكسيد المولبدنم تتراوح ما بين صفر% وحتى ٣٦%.

وقد تم استخدام حيود الأشعة السينية (XRD) ؛ الأشعة تحت الحمراء (IR)؛ مساحة السطوح و حجم المسام و تفاعل السيكلوهكسين لدراسة الخواص الفيزيوكيميائية والنشاطية الحفزية لعينات الحفازات المحضرة. كما تم قياس سعة الانتشار (dispersion capacity) لاوكسيد المولبدنم (MoO_3) علي سطح الالومينا بواسطة حيود الأشعة السينية الكمية (XRD quantitative phase analysis) ومساحة سطح الحفاز النوعية (Specific surface area). وأشارت النتائج إلي أن سعة الانتشار

(Dispersion capacity) لاوكسيد المولبدنم (MoO_3) علي سطح الالومينا حوالي ٤,٩٥ ذرة مولبدنم لكل نانومتر مربع.